Results in Engineering 30 (2026) 110648

Contents lists available at ScienceDirect

Results in Engineering

journal homepage: www.sciencedirect.com/journal/results-in-engineering

Research paper

Highly effective antimicrobial surface modification of polylactide prepared by supercritical fluid technology

Jakub Zágora [a,b], Zuzana Rybková [a,c,*], Kateřina Škrlová [d], Kateřina Malachová [a,c], Alexandra Muñoz-Bonilla [e], Marta Fernández-Garcia [e], Daniela Plachá [d,f,*]

[a] Nanotechnology Centre, CEET, VŠB–Technical University of Ostrava, 17. listopadu 2172/15, 708 00 Ostrava Poruba, Czech Republic
[b] Faculty of Materials Science and Technology, VŠB–Technical University of Ostrava, 17. listopadu 2172/15, 708 00 Ostrava Poruba, Czech Republic
[c] Department of Biology and Ecology, Faculty of Science, University of Ostrava, Chittussiho 10, 710 00 Ostrava, Czech Republic
[d] Department of Chemical Biology, Faculty of Science, Palacký University Olomouc, 17. listopadu 1192/12, 779 00 Olomouc, Czech Republic
[e] Institute of Chemistry and technology of Polymers, ICTP-CSIC, Juan de la Cierva 3, 28000 Madrid, Spain
[f] CATRIN – RCPTM, Palacký University Olomouc, Šlechtitelů 241/27, 779 00, Olomouc Holice, Czech Republic

ARTICLE INFO

Keywords:
PLA
Supercritical fluid technology
Impregnation
Cationic polymers
Antimicrobial surface modification

ABSTRACT

Antimicrobial surface treatment has emerged as an effective strategy to control microbial growth and mitigate infection spread across various materials, including plastics, metals, and textiles. These modifications enhance hygiene, extend material lifespan, and reduce environmental impact by lowering the need for frequent cleaning and disinfection. Their application spans healthcare, food production, and industry due to their ability to inhibit bacteria, fungi, and viruses. A variety of materials and methods are used to produce these modifications, with supercritical fluid technology (SFT) gaining prominence for its high efficiency and eco-friendliness. This study focuses on developing an antimicrobial surface by integrating poly[3-butyl-5-(2-methacryloyloxy)ethyl]-4-methylthiazol-3-ium iodide (PMTABul) with polylactide (PLA) using SFT. The resultant blend was characterized using spectroscopic, morphological, and thermal analysis techniques. Antimicrobial efficacy was assessed against bacterial strains *Acinetobacter baumannii, Escherichia coli, Staphylococcus aureus*, and methicillin-resistant *Staphylococcus aureus* (MRSA), demonstrating significant inhibition of biofilm formation (80–90%) and potential for broad-spectrum antimicrobial applications.

1. Introduction

Antimicrobial coatings or surface treatment have become increasingly popular in recent years as a solution for controlling microbial growth and the spread of infections. They are used on a wide range of materials, including plastics, metals, textiles, and others. Their advantage primarily lies in their ability to prevent microbial growth on surfaces, which helps to prevent infections and increase hygiene. Additionally, they can also extend the lifespan of materials such as textiles and plastics, reduce the need for frequent cleaning and disinfection, and thereby reduce costs and the burden on the environment [1]. According to their structure and composition, they can prevent the spread of bacteria, fungi, and viruses, thereby improving hygienic conditions in many sectors such as healthcare, food production, and industry [2]. In medicine, they are used as a protection against infections, particularly on contact surfaces such as catheters, probes, and other medical devices, reducing the risk of infection transmission to patients, limiting the need for antiseptics, and improving the overall health of patients [3,4].

Antimicrobial surface modifications are typically based on inorganic agents (e.g., silver or other metal-based systems), organic biocides, or intrinsically antimicrobial polymers, most frequently cationic polymers bearing quaternary onium groups, which can disrupt bacterial membranes and suppress early biofilm development [5–8]. On polymer substrates, antimicrobial surface modifications are commonly prepared by covalent grafting or surface-initiated polymerization, layer-by-layer assemblies, plasma/UV activation followed by coupling, or by physical incorporation/impregnation of the active agent into the near-surface region [9,10]. Chemical treatment based on silver ions or various types of nanomaterials, such as zinc oxide, copper, or silver

Raw data in Zenodo repository: 10.5281/zenodo.12934250

* Corresponding authors.
E-mail addresses: zuzana.rybkova@osu.cz (Z. Rybková), daniela.placha@upol.cz (D. Plachá).

https://doi.org/10.1016/j.rineng.2026.110648
Received 26 November 2025; Received in revised form 14 April 2026; Accepted 20 April 2026
Available online 21 April 2026

nanoparticles, have been also commonly used [2,5]. They are often manufactured using techniques such as electrodeposition, surface treatment, or supercritical fluid technology, when the supercritical CO_2 processing represents a solvent-free route [11–16].

Supercritical fluid technology (SFT) is becoming an increasingly popular method for antimicrobial coatings production and surface treatment due to its high efficiency and broad-spectrum effectiveness. The basic principle of this method involves the use of supercritical fluids, which are in a state between liquid and gas. These fluids are maintained at high pressure and temperature and can easily penetrate the surface of materials, allowing for even and consistent distribution of modifiers, in our case antimicrobial agents [9].

Coatings and surface treatment prepared using SFT can provide more effective protection against a range of harmful microorganisms, reduce the risk of infection and improve patient outcomes [7,17]. SFT allows the incorporation of high concentrations of antimicrobial agents into such coatings further enhancing their effectiveness. Another benefit of SFT is the ability to produce coatings and surface treatment with controlled release properties. This means that the release of antimicrobial agents can be regulated, allowing for sustained protection against harmful microorganisms over time [18]. Moreover, it is a relatively environmentally friendly non-toxic production method that does not produce hazardous waste or by-products, as no hazardous solvents are used [19]. Thus, the main advantage of using SFT compared to conventional methods is the elimination of hazardous solvents and the reduction of heating energy consumption in traditional processes, as supercritical solvents, especially CO_2, can be used from 28 °C.

In general, a great advantage of SFT is that it can be used in several different modes, which allow the processing of substances of different polarity even using non-polar CO_2, or allows the use of another supercritical fluid (e.g. water). There are many possible combinations that allow you to "tailor" the conditions of the SFT process and thus optimize the entire preparation process and obtain a product with the desired properties without negative effects on the environment.

Polylactide (PLA), a biodegradable and biocompatible polymer, has been widely used as matrix for antimicrobial composites and blends due to its environmentally friendly nature, its biodegradability and biocompatibility, which reduces the negative impact on the environment compared to traditional synthetic polymers. These materials are able to inhibit the growth of microorganisms and also provide a potential solution to the problem of antimicrobial resistance since their mechanisms of action could not develop resistance [20].

Currently, research is underway to produce PLA-based materials that is coated or modified with another antimicrobial polymer, such as poly [3-butyl-5-(2-methacryloyloxy)ethyl]−4-methylthiazol-3-ium iodide, abbreviated as PMTABul. PMTABul belongs to the category of heterocyclic polymethacrylates, which are cationic polymers with high stability and antimicrobial properties. These properties make heterocyclic polymethacrylates potentially important materials for many applications, including medical devices, food and cosmetic packaging, and construction materials [21–23].

PLA can be advantageously used as packaging material in hospitals. In such applications, amorphous PLA and semicrystalline PLA fulfil different roles due to their differing properties. Amorphous PLA, with its flexibility and optical clarity, is ideal for disposable items such as transparent packaging films, blister packs for medical devices, and short-term storage containers. Its lower processing temperatures and faster degradation rate make it suitable for applications requiring ease of handling and rapid turnover. Conversely, semicrystalline PLA, with its higher mechanical strength and thermal resistance, is preferred for durable packaging solutions that need to withstand sterilization processes and maintain structural integrity over time, such as reusable containers and protective casings for sensitive medical instruments [24]. These complementary applications ensure that both forms of PLA effectively contribute to the diverse needs of hospital biomedical packaging and can be made more effective by protective coatings with antimicrobial properties [25].

This study deals with the preparation of PMTABul polymer according to the literature [21] and its subsequent application on a support prepared from PLA. Our resulting material PLA+PMTABuI was prepared using supercritical fluid technology, without using any organic solvents or even water, and was subsequently characterized by common chemical-physical methods, along with antimicrobial properties, which were tested using bacterial gram-negative (G-) strains *Acinetobacter baumannii* and *E.coli*, and gram-positive (G+) strains *Staphylococcus aureus* and methicillin-resistant *Staphylococcus aureus* (MRSA). These opportunistic pathogens cause a wide range of infections and are responsible for the formation of biofilms that increase multidrug resistance and are proportionally represented in nosocomial infections that are associated with healthcare in healthcare facilities [26,27]. The aim of the work was to develop a material with potential use as a packaging in biomedicine, using a simple preparation method with a coating material and a polymer base on which the coating is applied.

2. Materials and methods

2.1. Materials

The following chemicals were used to prepare the polymer: 5-(2-hydroxyethyl)-4-methylthiazole (> 98%), methylsulfonyl chloride (MsCl) (> 99.7%), 4-dimethylaminopyridine (DMAP) (>99%), sodium bicarbonate ($NaHCO_3$), magnesium sulphate, anhydrous ($MgSO_4$), sodium azide (NaN_3), ethyl acetate (EtOAc), 1-iodobutane - (>99%), 2-methylpropenoic acid, distilled (>99%), N,N′-dicyclohexylcarbodiimide (DCC) (>99%), potassium hydroxide (KOH). All these compounds were supplied by Sigma-Aldrich, Co. The following chemicals were also used: anhydrous dichloromethane (CH_2Cl_2) (>99+%), triethylamine (TEA) distilled over potassium hydroxide (KOH) (>99%), anhydrous N,N-dimethylformamide (DMFA) (>99.7%), anhydrous dimethylsulfoxide, (DMSO) (>99.8%), methanol (MeOH) (>99,8%), ethanol (EtOH) (>99,8%), hexane (>96%), acetonitrile (CH_3CN) (>99.8%), azobisisobutyronitrile, twice recrystallized in MeOH (AIBN) (>98%). All these compounds were supplied by Thermo Scientific™. It was also used for sample preparation: carbon dioxide (CO_2) (4.8) (SIAD). Polylactide (PLA) IngeoTM 4032D was supplied by RESINEX Czech Republic s.r.o. The basic properties of the PLA used: density 1.24 g/cm^{3}and its average molecular weight in weight (M_w) is 182,000 Da.

2.2. Microbial strains

Potentially pathogenic strains *Acinetobacter baumannii* (*A. baumannii* CCM7117), *E.coli*(*E. coli*CCM3988), *Staphylococcus aureus* (*S. aureus* CCM4223) and methicillin-resistant *S. aureus* (MRSA CCM7111) were obtained from the Czech Collection of Microorganisms (Brno, Czech Republic). Bacterial strains were cultured at 37 °C on the plates with tryptone soya agar (HiMedia, India).

2.3. Preparation of antimicrobial polymer PMTABul for coating

PMTABul was prepared in several intermediate steps that included the preparation of 2-(4-methylthiazol-5-yl)ethyl methanesulfonate (M1), 5-(2-azidoethyl)-4-methylthiazole (M2), 2-(4-methylthiazol-5-yl) ethyl methacrylate (MTA), poly[2-(4-methylthiazol-5-yl)ethyl methacrylate] (PMTA). Briefly, 2-(4-methylthiazol-5-yl)ethyl methanesulfonate (M1) was prepared in a 500 mL flask under argon, 5-(2-hydroxyethyl)-4-methylthiazole (62.7 mL, 534 mmol) and anhydrous CH_2Cl_2 (250 mL) were stirred at 0 °C. TEA (78 mL, 593 mmol) was added, followed by MsCl (43 mL, 593 mmol) dropwise over 60 min. The mixture was stirred at room temperature for 4 h, diluted with $NaHCO_3$ solution, and extracted with CH_2Cl_2. The organic phase was dried over $MgSO_4$, and the solvent was removed. The orange mixture (117.2 g, 99% yield) was designated M1. M2 was prepared as: M1 (100.0 g, 452 mmol)

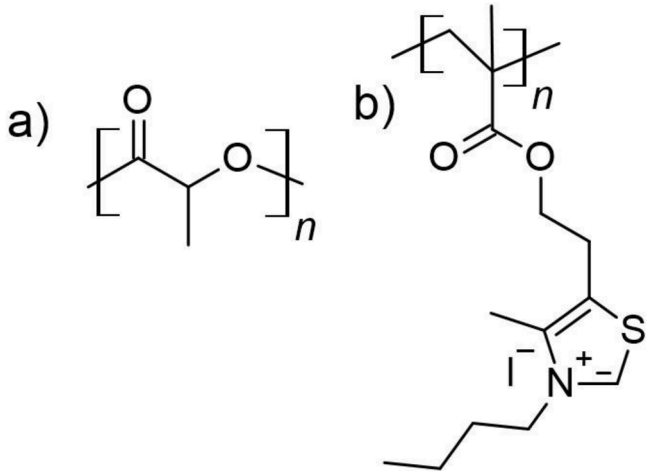

Fig. 1. a) Polylactide and b) PMTABuI structures.

Table 1
Prepared samples (measured on analytical balance Sartorius Tecator 6110 Balance, 0.0001 g, instrumental error ±0.00006 g).

Sample	Weight of PMTABuI (mg)	Increase of weight (%)	n (PMTABuI) (μmol)	n (PMTABuI)/ n (PLA) (mol %)
PLA (0 wt.%)	-	-	-	-
PLA+PMTABuI (0.5 wt.%)	0.4	0.10 ± 0.06	0.25	0.02
PLA+PMTABuI (2 wt.%)	8.1	2.70±0.02	27.07	0.49
PLA+PMTABuI (4 wt.%)	4.5	5.10±0.05	13.913	0.93
PLA+PMTABuI (5 wt.%)	16.1	5.35±0.02	41.24	0.98
PLA+PMTABuI (10 wt.%)	23.4	7.94±0.03	42.25	1.45
PLA+PMTABuI (20 wt.%)	45.3	3.53±0.03	16.19	0.64

and anhydrous DMFA (1000 mL) were mixed under argon, and NaN_3 (73.5 g, 1130 mmol) was added in portions. The mixture was stirred at 70 °C for 4 h, cooled, and the solvent evaporated. The resulting mixture was dissolved in EtOAc/H_2O (1:1), separated, washed, and dried over $MgSO_4$. The remaining solvent was removed, and the orange oil was purified by chromatography to yield yellow oil M2. MTA was prepared by mixing 5-(2-hydroxyethyl)-4-methylthiazole (40.9 mL, 350 mmol), DMAP (4.2 g, 35.0 mmol), 2-methylpropanoic acid (38.4 mL, 454 mmol), and anhydrous CH_3CN (175 mL) with DCC (94.0 g, 454 mmol) in CH_3CN (225 mL). The mixture was purified by chromatography, yielding yellow oil MTA (68.8 g, 93%). PMTA was synthesized from MTA (10.6 g, 50 mmol) and AIBN catalyst (410 mg, 2.5 mmol) in 50 mL of dry DMSO. The mixture was purified by chromatography and precipitated in EtOH. The precipitate was filtered, vacuum dried, yielding PMTA (9.9 g, 91%). PMTABuI was prepared from PMTA1 (1.0 g, 5 mmol) and 1-iodobutane (2.1 mL, 18 mmol) in 50 mL of dry DMF. After precipitation in EtOH, the yellow-white precipitate was vacuum dried, yielding PMTABuI (1.6 g, 93%). The polymer was synthesized accordingly to procedure described in the literature [21]. The prepared PMTABuI was subsequently applied to the surface of polylactide (PLA) by the SFT method. Fig. 1 shows the formulas of both polymers used - a) polylactide, b) PMTABuI.

2.4. Preparation of antimicrobial surface modification

Firstly, PLA films were prepared using a Collin 200 × 200 press under the following conditions: temperature of 190 °C (above the melting temperature of PLA), pressure of 0.1 MPa for 2 min (heating and melting), 1 MPa for 3 min (pressing), and 1 MPa for 2 min (cooling). The final thickness was 0.2 mm.

Supercritical fluid process was performed using device Spe-ed™ SFE-4 from company Applied Separations. Conditions for supercritical surface treatment were selected based on previous repeated experiments with the solubility of PMTABuI and PLA in supercritical carbon dioxide (SC—CO_2). All samples were prepared under the same conditions: temperature (60 °C), pressure (20 MPa), reaction time (3 h), and depressurization flow (1 L/min). The original films were cut into uneven strips with a width of 1.5 cm and length approx. 3 cm. These strips were then weighed (weights ranged from 200 to 350 mg) and placed into a reaction cartridge, where the calculated amount of PMTABuI was added. The prepared samples were designated as PLA+PMTABuI (x wt.%), where x corresponds to the calculated weight percentage of PMTABuI in blends with PLA, x = 0, 0.5, 2, 4, 5, 10 and 20. Changes in weights before and after treatment of PLA films are presented in Table 1. The significant difference between the loading of PMTABuI in the PLA+PMTABuI (2 wt. %) and PLA+PMTABuI (4 wt. %) samples is due to the significantly different weight of the prepared PLA strips.

2.4.1. Methods of characterization

The samples were characterized using infrared spectroscopy (FTIR, Nicolet iS50), measured on an attenuated total reflectance (ATR) diamond crystal, with 62 scans in the mid-infrared spectrum (400 - 4000 cm^{-1}), and baseline corrected in the OMNIC program. Scanning electron microscopy (SEM) JEOL JSM-7610F Plus (JEOL, Japan) with an auto emission source was used to study the morphology of the samples. The element composition of the samples and the stability of modification and films were also investigated by SEM/EDAX method. The samples were examined at accelerating voltages of 3 and 20 keV using secondary electron detection. For sputtering, the Quorum Q150V ES plus was used with 2 nm gold coating and 30 mA current. For surface topography evaluation, the samples were measured using atomic force microscopy (AFM) on a LiteScopeTM device in contact mode, with a measurement area of 20 × 20 μm in the x and y directions. X-ray diffraction (XRD) spectra were obtained using a RIGAKU X-ray system with a Cu lamp (energy 8.04 keV, wavelength 0.15406 nm), operating at 40 kV and 40 mA, with a K-β filter and a scintillation detector. Thermogravimetric analysis (TGA) was performed using a TGA/STA-FTIR-MS SETARAM system from 30–800 °C with a temperature ramp of 10 °C/min in an argon atmosphere. Differential scanning calorimetry (DSC) was performed using a DSC200 TA instrument with an intracooler, over a temperature range of −20 °C to 200 °C, with a heating rate of 10 °C/min. ^1H NMR spectra of quaternized polymer was recorded in DMSO-d6 with a Bruker AVANCE III HD-400AVIII spectrometer operating at 300 MHz. The distribution of molecular weights of the unquaternized polymer was measured by GPC using a chromatographic system Waters Division Millipore equipped with a refractive-index detector (Waters model 410). Dimethyl formamide (99.9%, Aldrich) containing 0.1% of lithium bromide (≥99%, Aldrich), was used as the eluent at a flow rate of 1 mL/min at 50 °C. Styragel packed columns (HR2, HR3, and HR4, Waters Division Millipore) and poly(methyl methacrylate) standards (Polymer Laboratories, Ltd.) between 2.4·106 and 9.7·102 g/mol were used. Contact angle was evaluated by device Data Physics OCA 15 EC/B, using demineralised water (Milliq, 18.2Ω), dosage 3 μl and captured on camera BU205M with high performance upgrade UPHSV 205.

2.5. Detection of inhibition of biofilm formation

Since the standard agar disk method did not show a difference between samples and all samples showed growth inhibition only under the disk, the following test was used to determine antimicrobial inhibitory effects of PLA+PMTABuI composites on biofilm formation, which was assessed using the Crystal violet biofilm assay [28–30]. PLA and its composites (PLA+2% PMTABuI, PLA+5% PMTABuI, PLA+10%

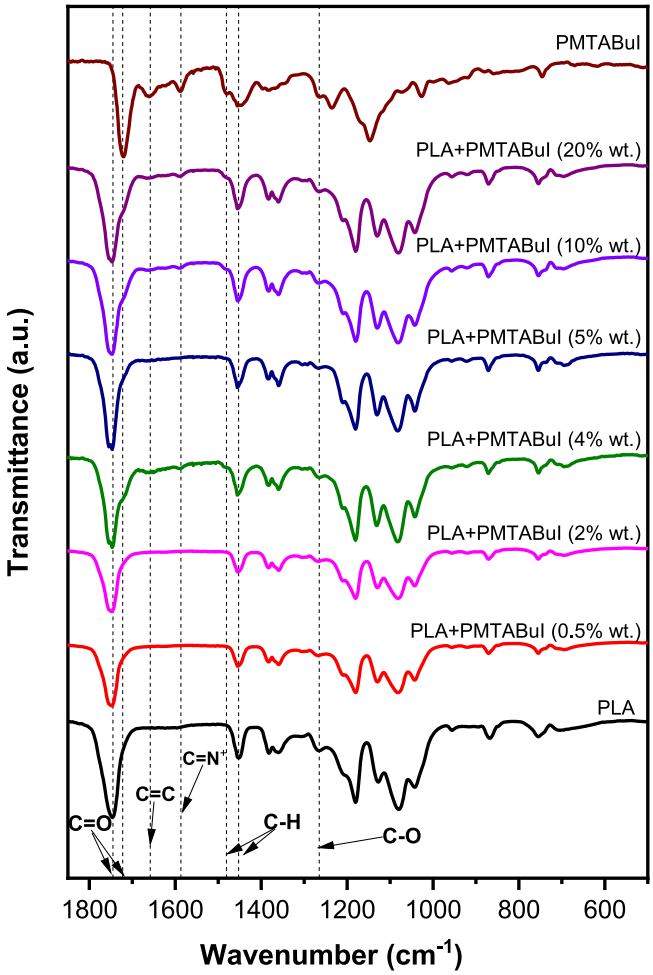

Fig. 2. ATR-FTIR spectra of prepared PLA+PMTABuI films.

PMTABuI) were cut into 6 mm diameter discs. Bacterial strains were inoculated into 10 mL of tryptone soya broth (TSB, HiMedia, India) and cultured overnight at 37 °C. After overnight incubation, microbial suspensions were standardized with TSB to a concentration of 1×10^5 CFU·mL^{-1}. Discs of PLA and its composites were placed in the wells of 96-well microplates (1 disk/well). A volume of 200 μL of the prepared inoculum was added to each well. The plates were statically incubated at 37 °C for 24 h. The culture medium was gently aspirated and each one was properly washed with 200 μL of deionized water. The microplates were dried at 60 °C for 15 min. Then, the biofilms were stained with 200 μL of 0.1% crystal violet (Sigma-Aldrich, USA) at room temperature for 20 min. Then the samples were washed three times with deionized water to remove an unbound dye and were dried afterwards at 60 °C for 15 min. After drying, the crystal violet was solubilized in 200 μL of 96% ethanol while shaking (ELMI orbital shaker DOC-20 L, Latvia) at room temperature for 20 min. Finally, 150 μL of the crystal violet solution was transferred into a new 96-well microplate, and the absorbance was measured using a microplate spectrophotometer (Epoch, BioTek, USA) at a wavelength of 584 nm. The total amount of biofilm was directly proportional to absorbance values of the crystal violet solution. The results were calculated as a percentage of biofilm reduction. Also, all viable cells in biofilm were quantified by the MTT cell viability assay [31]. After treating composites with bacterial strains, the planktonic bacteria were discarded and 200 μL of 0.5 mg·ml^{-1} 3-(4,5-dimethylthiazol-2-yl)-2,5-diphenyltetrazolium bromide (Sigma-Aldrich, USA) was added. The plates were incubated at 37 °C for 2 h. Subsequently, the MTT was aspirated and 200 μL of dimethyl sulfoxide (VWR International, Czech Republic) wad added. The result solution was used for an absorbance measurement at 570 nm. Each sample was tested in six replications. Statistical analysis was performed using one-way ANOVA with Tukey's multiple comparison test, $p \leq 0.05$ was considered significant.

2.6. Stability of modified surface

The stability of the modified surfaces of the prepared samples was investigated by immersing the coated films in glass vials with various media. These medias were the air, distilled water, NaCl solution (10 wt. %) and PBS buffer (pH 7.4). The samples were immersed for 72 h, then removed from the medium and dried. Changes in surface composition were observed using SEM/EDAX.

3. Results and discussion

The prepared samples and their starting materials were subjected to chemical and physical characterizations using FTIR, SEM, SEM/EDAX, AFM, XRD, TGA and DSC. Changes in crystallinity were observed by XRD and DSC, surface morphology by SEM and AFM and amount of polymer and its bonding by TGA and FTIR. The inhibitory effect of PLA and PLA+PMTABuI films on biofilm formation was assessed using the crystal violet biofilm assay on *A. baumannii, E. coli, S. aureus*, and methicillin-resistant *S. aureus*, which are considered important causative agents of nosocomial infections in healthcare facilities.

The average molecular weight (M_n) and polydispersity index (PDI) of

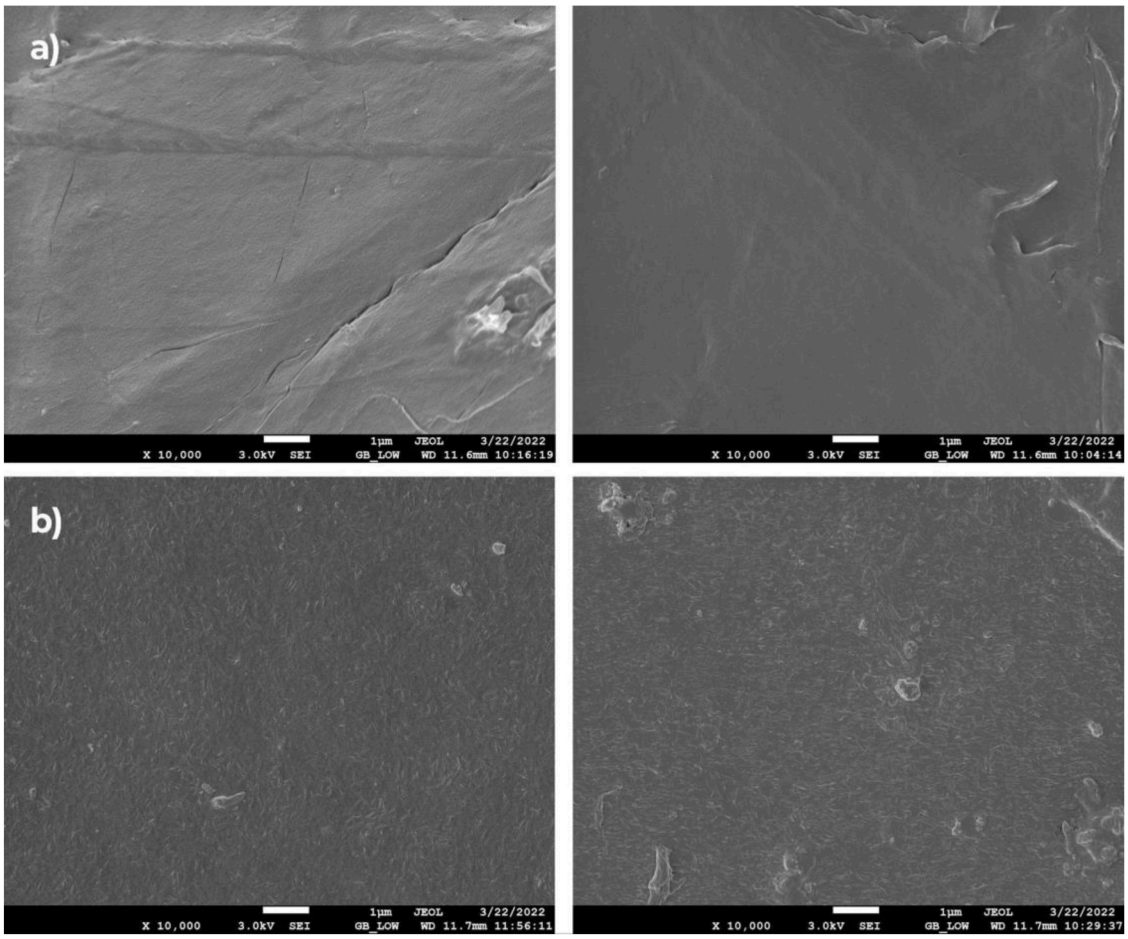

Fig. 3. SEM pictures of a) pure PLA, b) PLA after supercritical treatment (the two images were chosen from distinct areas on the sample for enhanced surface visualisation).

the synthetized polymer before and after quaternization were determined by GPC. The prepared PMTA reached M_n 36,000 Da and PDI was 1.9, after quaternization an M_n (PMTABuI) of 68,800 Da was achieved. The average molecular weight (M_w) of commercial PLA was determined in our previous work to be 182,000 Da [17]. The structure of PMTABuI was confirmed by ^{1}H NMR, the results of the determination are presented in the appendix, see Fig. S1, where characteristic groups and the presence of quaternized nitrogen are evident.

All other results already compare PLA and PMTABuI polymers before and after SFT processing. The amounts of PMTABuI applied to the PLA surface are documented in Table 1, which shows the added amount of PMTABuI as a surface modifier to the reaction cartridge for each sample and then the determined amount of PMTABuI actually deposited after the SFT processes. .As can be seen from Table 1 (Section 1.3), no changes in weight were detected for pure PLA (no PMTABuI was added to the cartridge). With increasing PMTABuI content during the reaction, a loss of process efficiency can be observed due to changes in equilibrium conditions. The reason for these losses is probably the partial precipitation of PMTABuI on the walls of the reaction cartridge, which occurred at a higher PMTABuI content while maintaining the same pressure, temperature and cartridge volume in the system. Moreover, at a higher amount of PMTABuI, the SC—CO_2 saturation endpoint was reached. This is manifested as less efficient impregnation at 10 wt. % and ineffective impregnation at 20 wt. %.

ATR-FTIR spectroscopy was used to confirm the presence of PMTABuI on PLA films. The spectra of all films in the range of 1800 - 550 cm^{-1} are shown in Fig. 2. For PLA, the characteristic peaks include the carbonyl stretching vibration (C = O) at 1745–1751 cm^{-1}, deformation of the -CH_3 bond at 1454 cm^{-1}, the -C-O—C bond at 1265–1027 cm^{-1}, and the C—C bond at 867 cm^{-1} [32]. For PMTABuI, the characteristic absorption bands include the carbonyl stretching vibration (C = O) at 1718 cm^{-1}, C = C band at 1660 cm^{-1}, thiazolium vibration C = N$^+$ at 1587 cm^{-1}, deformation of the -CH_3 bond at 1481 cm^{-1}, and the -C-O—C- bond at 1265, 1234, 1128, and 1039 cm^{-1} [33]. The presence of the C = N$^+$ bond at 1587 cm^{-1} indicates that PMTABuI is on the surface of PLA. This bond is already clearly visible in the spectrum of PLA+PMTABuI of 4, 10 and 20 wt. %.

To evaluate the surface morphology of the starting materials, characterization was performed using SEM analysis for pure PLA (before and after supercritical processing, see Fig. 3), prepared powdered PMTABuI (Fig. S3) and further prepared materials of PLA with PMTABuI after supercritical processing (Figs. 4 and 5). Fig. 3 shows changes in the surface morphology of PLA films, from non-processed PLA (Fig. 3a) with a smooth surface and minor defects, to processed PLA (Fig. 3b) with increased surface roughness due to the recrystallization process. This morphological change appears as flake-shaped structures on the surface. This observation was also confirmed by AFM, as will be discussed further. In Fig. S3, amorphous PMTABuI particles of various shapes and sizes from 1 to 500 μm are visible. Particles were created during precipitation and vacuum drying in the preparation process.

Figs. 4 and 5 show particles of PMTABuI on the surface of PLA films created by RESS mode of SFT. Visibly, size of these particles decreased during the SFT process and the change of shape of the particles occurred in several cases. Lower amount of the PMTABuI into the process created more smooth shaped particles. The best results in terms of surface coverage were shown when 20 wt. % of PMTABuI in the composite is

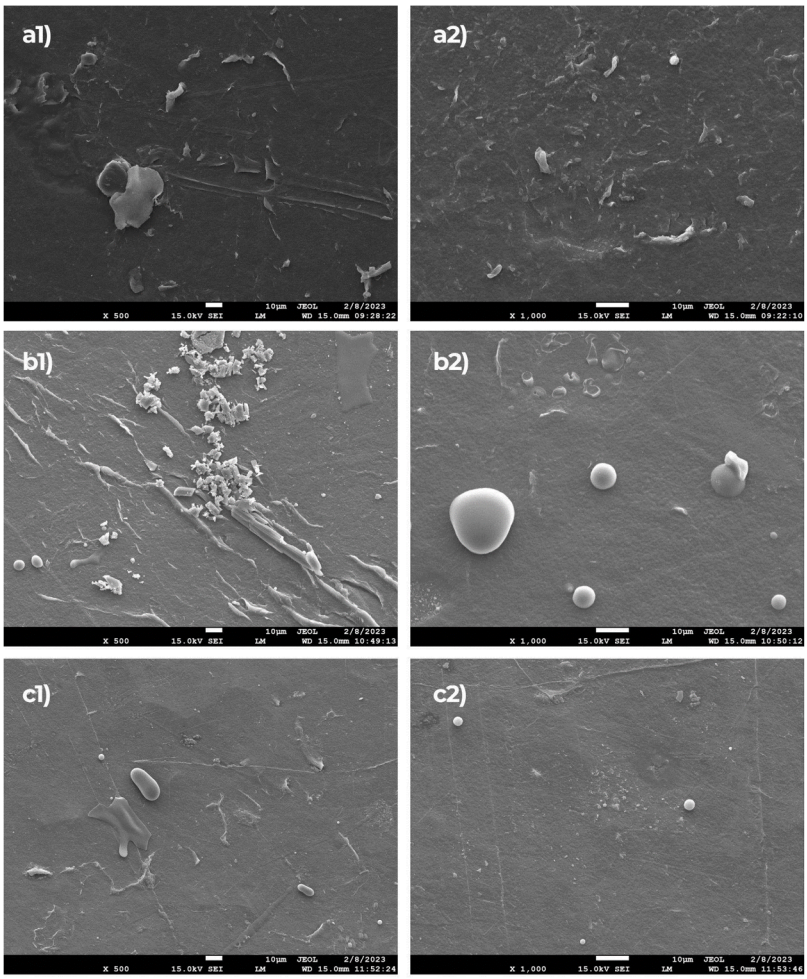

Fig. 4. SEM pictures of PLA+PMTABuI after supercritical treatment, a1) and a2) 0.5 wt. % at 500 × and 1000 ×, b1) and b2) 2 wt. % at 500 × and 1000 ×, and c1) and c2) 4 wt. % at 500 × and 1000 ×, respectively.

used. However, it caused severe defects on the surface of PLA films. A balance between coverage of the surface and creating only minor defects is found in composites with 2 wt. %, 4 wt. % and 5 wt. % of PMTABuI. The RESS process of SFT produced two types of particles on the surface of PLA films. These particles are spherical, with sizes ranging from 80 nm to 15 μm, or plate-like with fractured edges, with diameters from 1 to 50 μm.

SEM/EDX mapping was used to confirm that the particles on the PLA surface are composed of PMTABuI. Iodine was used as an indicator for the presence of PMTABuI, since another different element in PMTABuI compared to PLA polymer is nitrogen, which is difficult to detect due to its similarity to the surrounding elements (carbon and oxygen). Iodine, as the counterion of PMTABuI, was detected in samples with PMTABuI content higher than 1 wt. % due to the detection limit of the device, see Fig. 6.

The surface parameters were determined using AFM. These parameters, including R_a (average surface roughness) and R_z (distance between the highest and lowest points), are presented in Table 2. The evaluation of surface topography was chosen to better understand small changes in surface roughness. Surface roughness is one of the factors influencing the growth of microbial biofilm on a surface. In general, rougher surfaces are more conducive to biofilm formation. Thus, there may be a combined effect between a smoother surface and an antimicrobial coating [34,35].

The different R_z and R_a values for the individual samples in the Table 2 are clearly explained by Figs. 7 and 8, which show the inhomogeneities of the surfaces formed after SC—CO_2 treatment. In the case of pure PLA (Fig. 7), a change in surface roughness is evident after SFT, although the R_a value is lower than that of PLA before treatment. The effect of SC—CO_2 leads to the formation of deeper "holes" or pores on the PLA surface, which increase the R_z value. The surface of both samples is consistent with the morphology determined by SEM analysis.

In the case of PLA+PMTABuI composites, the changes in R_z were lower, except for PLA+PMTABuI (0.5 wt. %), probably due to the accumulation of PMTABuI particles in the pores formed by SC—CO_2 (see Fig. 8). In the case of PLA+PMTABuI (0.5 wt. %), the polymer covered only a part of the surface (see Fig. 8a), which led to an increase in the surface roughness R_a and a more pronounced difference in R_z. For samples with increasing PMTABuI content, the surface roughness, expressed as R_z, decreased and ranged from 387 to 736 nm, indicating some surface inhomogeneity for all samples. The R_a value (as shown in Fig. 8 and Table 2) also decreased compared to pure PLA and the sample PLA+PMTABuI (0.5 wt. %). The best performing sample was the PLA+PMTABuI (10 wt. %) sample (Fig. 8e), which showed the lowest R_a value and the lowest differences in R_z on the surface, indicating the most homogeneous surface. A certain exception was the PLA+PMTABuI (5 wt. %) sample, in this case probably due to the presence of larger particles, see Fig. 5d1.

The changes in the observed morphologies of the samples can be explained by the fact that surface impregnation with SFT occurs in such a way that SC—CO_2 partially dissolves PLA, thereby increasing its surface roughness. SC—CO_2 also dissolves PMTABuI. After depressurization of the system, PMTABuI precipitates on the PLA surface, which can be observed as a decrease in surface roughness with increasing content of

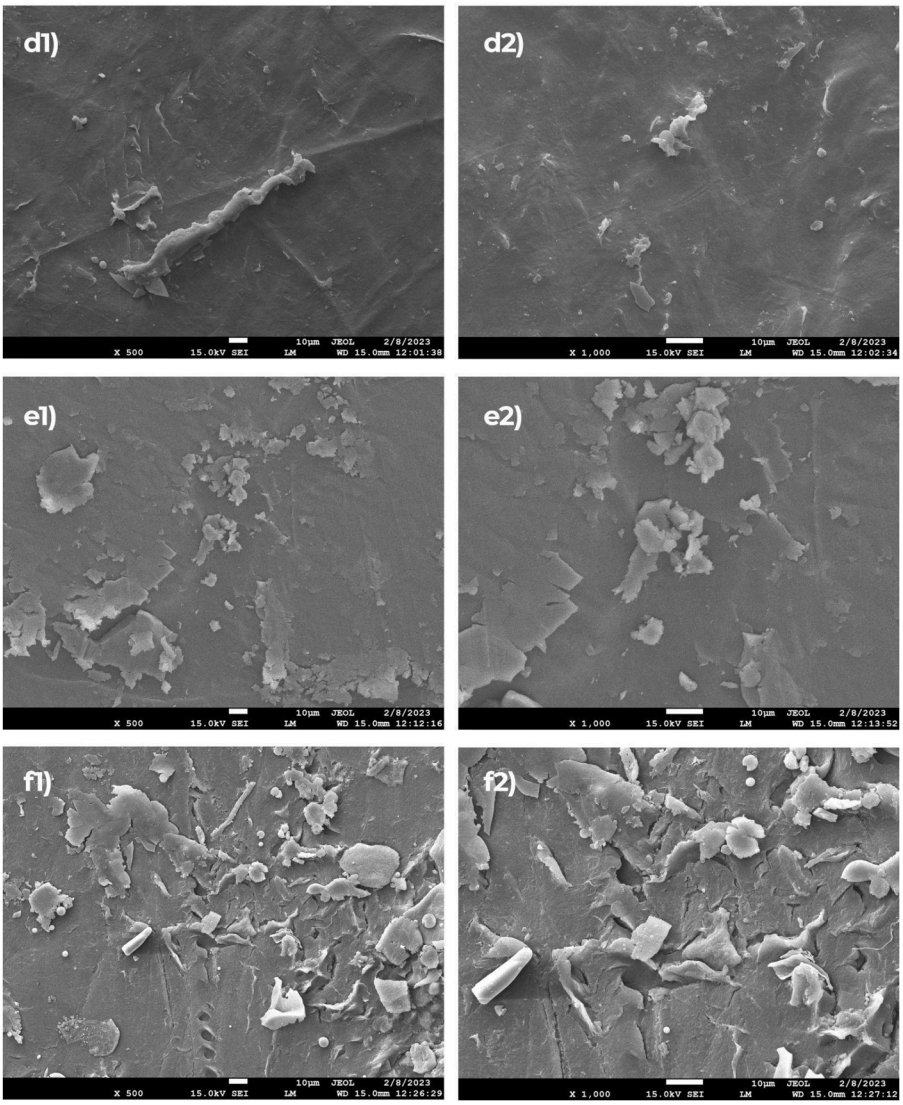

Fig. 5. SEM images of PLA+PMTABuI after supercritical treatment, d1) and d2) 5 wt. % at 500 × and 1000 ×, e1) and e2) 10 wt. % at 500 × and 1000 ×, and f1) and f2) 20 wt. % at 500 × and 1000 ×, respectively.

PMTABuI. PMTABuI also precipitates on the surface of the reaction cartridge. The dissolution of PLA and PMTABuI by SC—CO_2 was confirmed by analysis of extracts obtained after the supercritical process. The extracted particles were dissolved in ethanol and evaluated using STEM. All images can be seen in Fig. S3. The size of these particles ranges from 35 to 200 nm for PLA, with smaller particles agglomerating, and 18–80 nm for PMTABuI with similar agglomeration. In the case of PLA+PMTABuI, the particles form larger agglomerates of about 200 nm in size, which consist of particles similar to the molten particles.

Another characterization of the prepared samples was X-ray diffraction (XRD), which was used to study the effect of SFT on the crystallization of the materials (see Fig. 9). As mentioned in the Introduction, the amorphous or crystalline state determines the possible use of PLA in packaging materials. The PLA film is initially amorphous after pressing. However, it is seen that crystallization occurs from the beginning of the SFT process [32,33]. After 1 h of processing, a characteristic diffraction peak with high intensity at 16.9° and 19.1° corresponding to the (110)/(200) and (203) planes begins to appear. In addition, a diffraction peak with low intensity at 22.5° for the (015) plane continuously appears [28,34]. These peaks become more pronounced with time, but after 3 h, higher crystallinity is no longer noticeable, see Fig. 9a. Based on this, a time of 3 h was chosen for the SFT process.

The XRD patterns of the composites, PLA+PMTABuI are shown in Fig. 9b Based on the intensity and shape of the characteristic peaks, it is evident that the impregnation by PMTABuI, which is an amorphous polymer, reduces the crystallization capacity of PLA during the SFT process. At low amounts of PMTABuI, the crystallinity is practically unaffected, but with increasing amounts of PMTABuI, the crystallization of PLA is inhibited.

The thermal stability of composites was analysed by thermogravimetric analysis under inert atmosphere and at heating rate of 10 °C/min. Fig. 10 shows the TGA curves of PLA+PMTABuI composites along with pure PLA and PMTABuI polymers. All composite samples behave similarly to pure PLA, exhibiting only one degradation peak. The stability of the composites is slightly increased with the impregnation of PLA with PMTABuI, presenting values similar to those reported in the literature [20], though the effect is nearly negligible.

The thermal behavior of PLA, PLA (3 h), PMTABuI, PLA+PMTABuI (2 wt%), PLA+PMTABuI (10 wt%), and PLA+PMTABuI (20 wt%) was studied by DSC (see Fig. 11). PMTABuI is an amorphous polymer with T_g at 118 °C [36]. PLA film obtained from compression moulding presents the typical curve of the glass transition around 60 °C, followed of a wide range cold crystallization and then, the melting transition at around 168

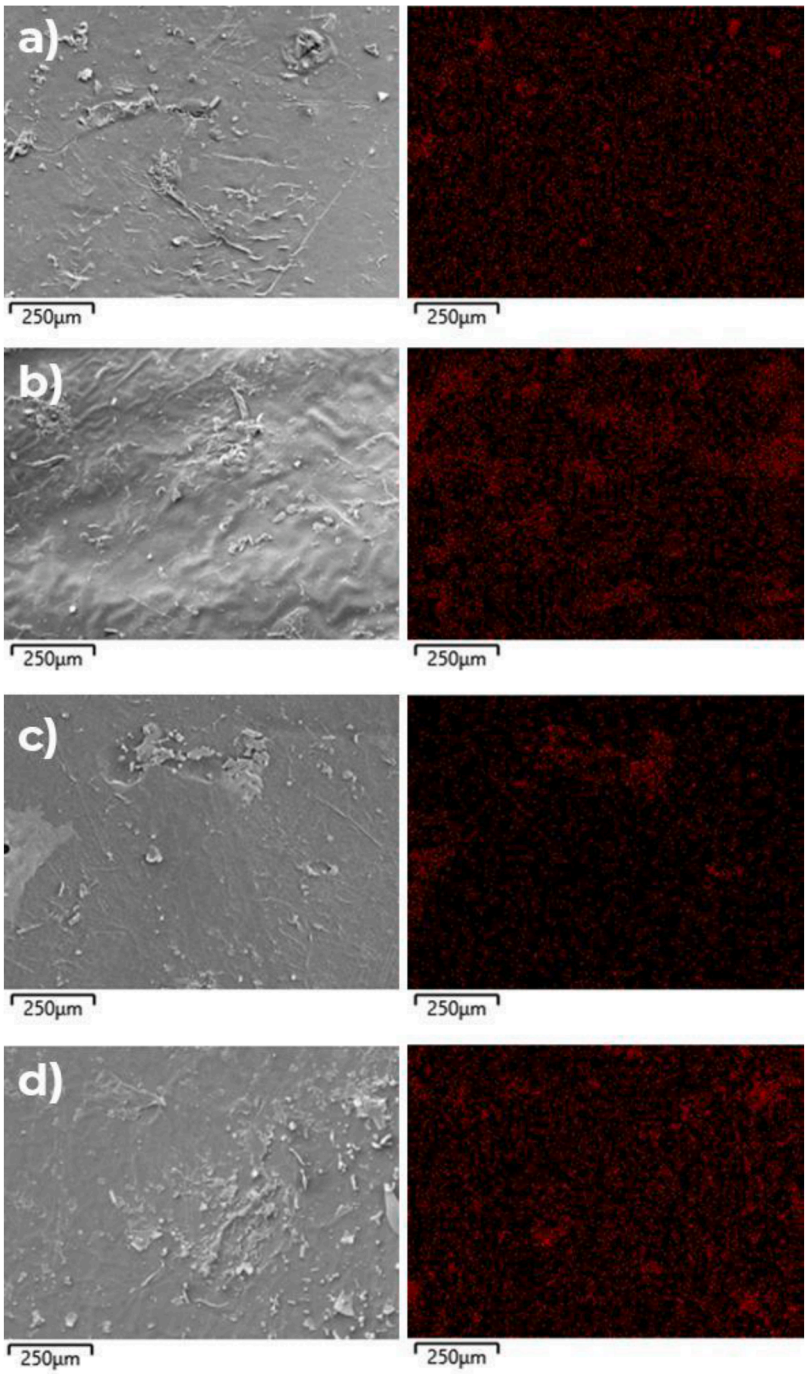

Fig. 6. EDX mapping of Iodine of PLA+PMTABuI films, a) 2 wt %, b) 5 wt %, c) 10 wt %, and d) 20 wt %.

Table 2
Surface roughness of samples.

Sample	R_z (nm)	R_a (nm)
PLA	333 ± 80	333 ± 33
PLA – 3 h SFT	925 ± 272	289 ± 105
PLA+PMTABuI (0.5 wt%)	1885 ± 438	729 ± 168
PLA+PMTABuI (2 wt%)	615 ± 145	215 ± 48
PLA+PMTABuI (4 wt%)	572 ± 145	195 ± 50
PLA+PMTABuI (5 wt%)	736 ± 368	291 ± 13
PLA+PMTABuI (10 wt%)	387 ± 120	140 ± 50
PLA+PMTABuI (20 wt%)	614 ± 213	184 ± 75

°C. The enthalpy of cold crystallization is 1.91 J/g while the melting is 1.99 J/g. The difference between these enthalpies gives the initial crystallinity of the film considering enthalpy of 100% pure PLA crystal is 93.6 J/g. PLA is practically amorphous, as observed by XRD (see Fig. 9). However, after 3 h of SFT processing, PLA crystallizes, showing a wider cold crystallization transition followed by melting of the crystals. The difference in enthalpy is 40.4 J/g, corresponding to approximately 43% crystallinity [37]. Coating with PMTABuI results in a slight reduction in crystallization enthalpy, with melting enthalpy values of 45.1, 41.8, and 36.7 J/g. In these cases, the cold crystallization process may overlap with the glass transition of PMTABuI, potentially leading to over- or underestimation of crystallinity. Nevertheless, the DSC results are in concordance with XRD observations, where the coating with large

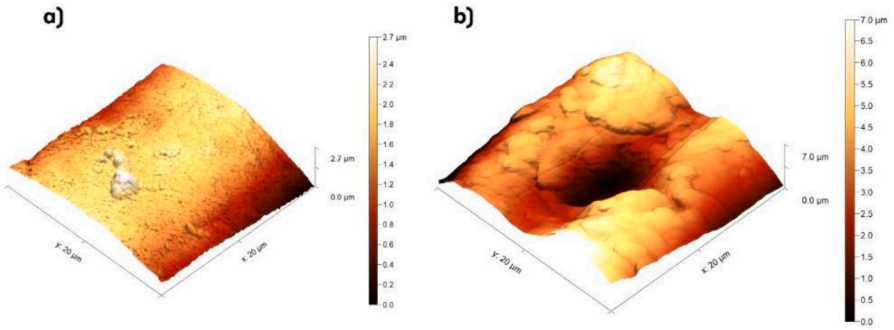

Fig. 7. AFM image of pure PLA film a) before and b) after supercritical fluid treatment.

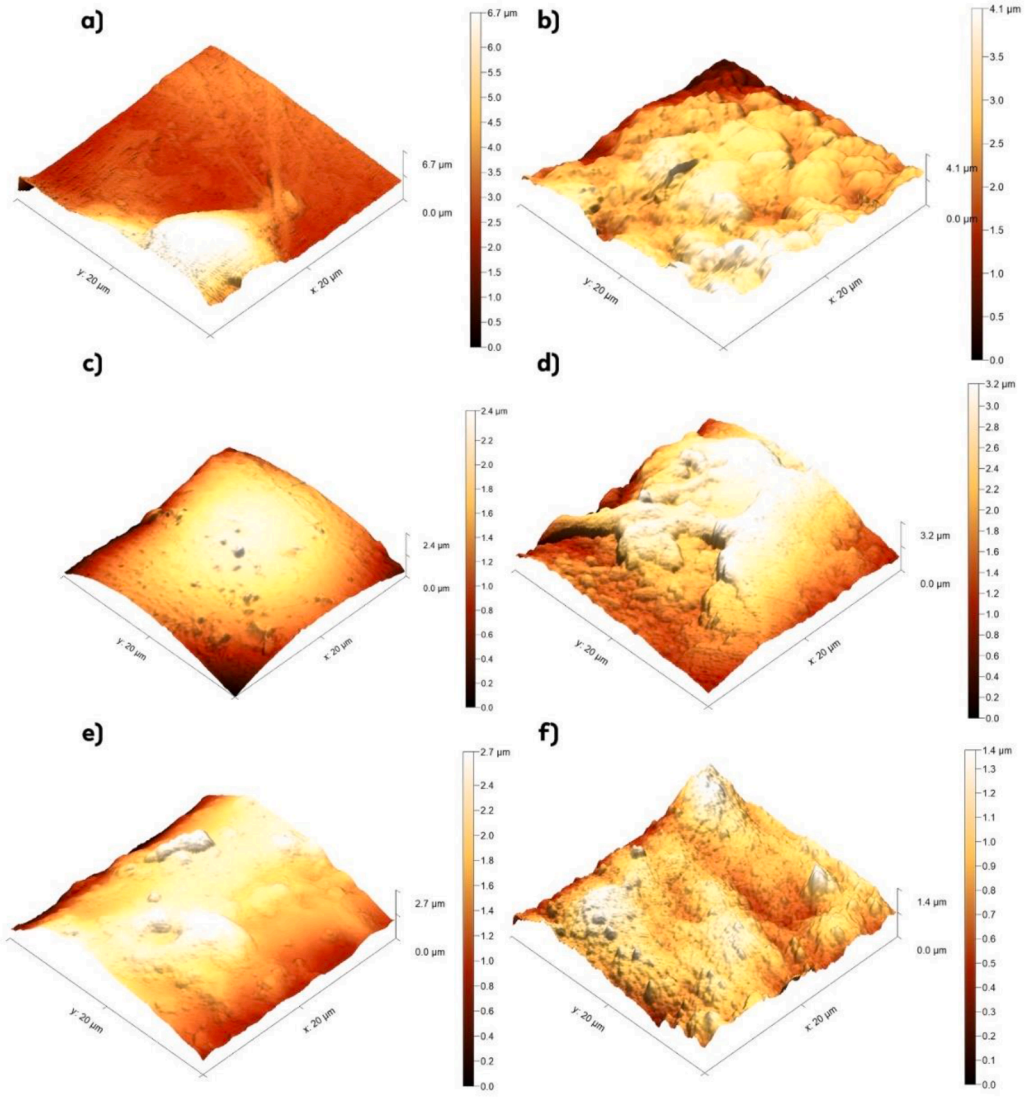

Fig. 8. AFM images of PLA+PMTABuI films, a) 0.5 wt. %, b) 2 wt. %, c) 4 wt. %, d) 5 wt. %, e) 10 wt. %, and f) 20 wt. %, respectively.

amount of antimicrobial PMTABuI diminishes PLA crystallinity.

To verify the hydrophilicity/hydrophobicity, the surface tension and contact angle were measured for all prepared samples. Table 3 shows the samples obtained by drop analysis tested with water (see Fig. S4). The original PLA and PLA after SFT treatment (PLA-SFT) are on the border of hydrophobicity/hydrophilicity. No clear trend was observed for individual samples with increasing PMTABuI content, probably due to the inhomogeneity of the formed coatings, but the hydrophilicity of the samples increases after interaction with PMTABuI. This is due to the presence of antibacterial cationic polymer on the PLA surface.

3.1. *Antimicrobial effect of PLA+PMTABuI composites*

For antimicrobial test were chosen the sample PLA+PMTABuI (2 wt. %), PLA+PMTABuI (5 wt. %) and PLA+PMTABuI (10 wt. %) because they showed best homogeneity of covering the surface with PMTABuI. In

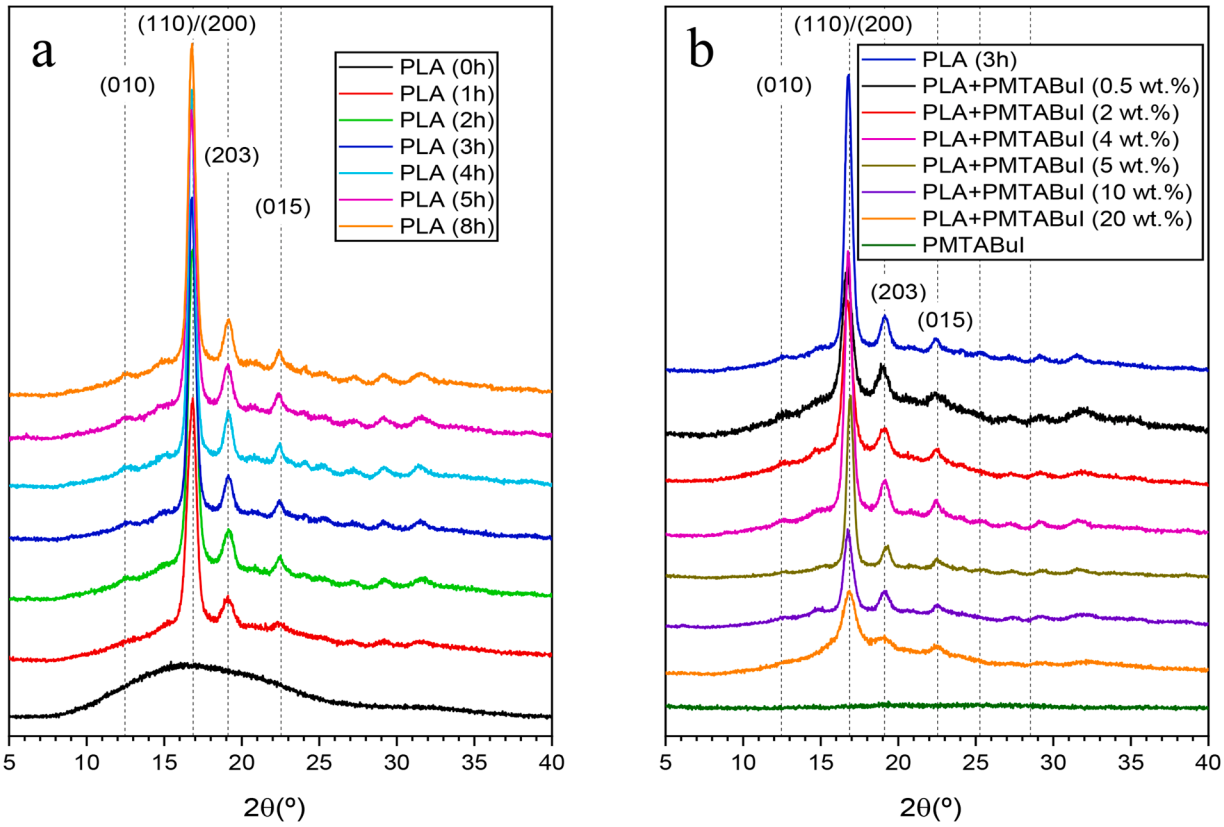

Fig. 9. XRD profiles of a) the original PLA film, PLA films after SFT and b) PMTABuI and composites of PLA+PMTABuI.

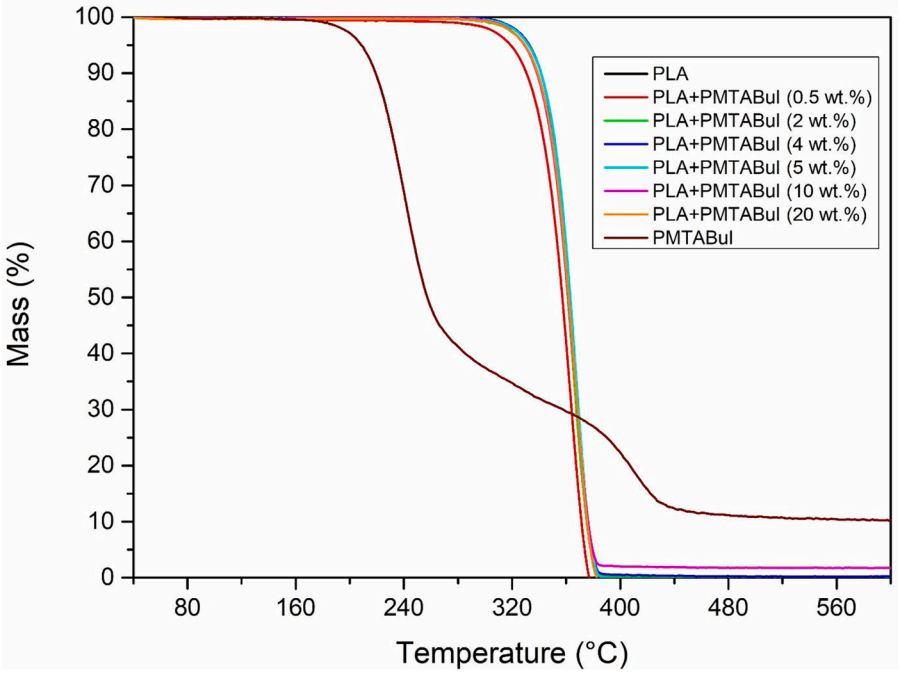

Fig. 10. TGA analysis of PLA, PMTABuI, and PLA+PMTABuI composites.

lower concentrations (<2 wt. %) the films did show uneven distribution. Similar effect occurred in 20 wt. % of polymer where the process was not efficient enough and distribution was also uneven.

The antimicrobial effect of PLA+PMTABuI was determined as an inhibitory effect on formation of bacterial biofilm *A. baumannii, E. coli, S. aureus* and MRSA (Fig. 12a). The specific structure of biofilms results in increased resistance of bacteria to antibacterial agents [38–40]. Biofilm formation was quantified using the Crystal violet microtiter plate assay [41]. Pure PLA was used as a negative control, demonstrating zero inhibitory effect on biofilm formation. For all evaluated PLA+PMTABuI

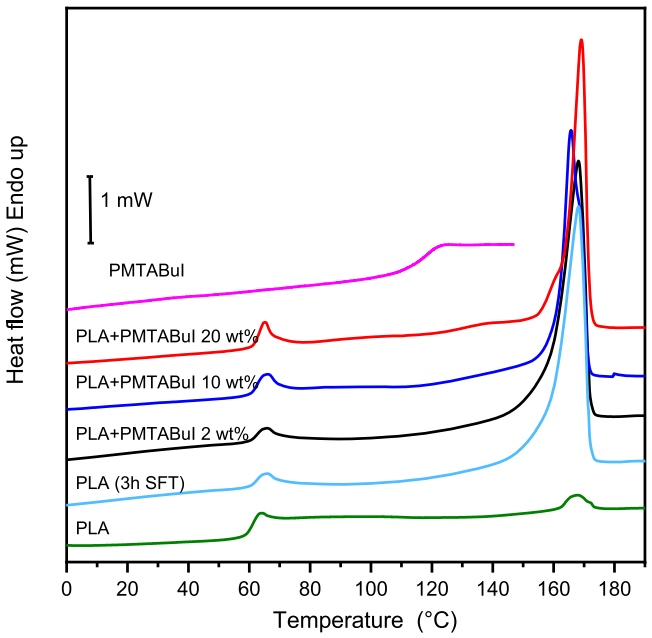

Fig. 11. DSC curves of PLA, PMTABuI, PLA after 3 h of SFT and PLA+PMTABuI (2, 10 and 20 wt. %).

Table 3
The contact angle values of all prepared samples.

Sample	Contact angle (°)
PLA	87.4 ± 0.1
PLA (3 h SFT)	79.5 ± 0.1
PLA+PMTABuI (2 wt. %)	62.1 ± 0.6
PLA+PMTABuI (4 wt. %)	44.9 ± 0.4
PLA+PMTABuI (5 wt. %)	68.3 ± 0.6
PLA+PMTABuI (10 wt. %)	56.4 ± 0.1
PLA+PMTABuI (20 wt. %)	74.0 ± 4.0

coatings (2, 5, 10 wt.%), a significant inhibitory effect on the formation of all four bacterial biofilms was found ($p < 0.05$) (Fig. 12a, Table S1). In the case of coating with 10 wt. % PMTABuI, the highest inhibitory efficacy was found for G^- strain of *A. baumannii* (90 ± 6%). The effect of inhibition *A. baumannii* biofilm is considerable important in the context of causing nosocomial and community-acquired infections, multi-drug resistance and ability to form biofilm in hospitals and the environment [42,43]. An inhibitory effect greater than 80% was also achieved for the G- strain of *E. coli*(83 ± 8%). Biofilm inhibition in G+ bacteria was 82 ± 4% for S. aureus and 77 ± 5% for MRSA. The difference in sensitivity between G- and G+ bacterial strains was not significant ($p > 0.05$) and may be related to variations in their surface structures and individual sensitivity of strains to PMTABuI. The outer membrane of G- bacteria is more complex because it contains lipopolysaccharides (LPS) while G+ bacteria have more simple membrane with teichoic and lipoteichoic acids [44,45]. The contribution of bacterial extracellular vesicles (BEVs) to biofilm stability is also discussed in the literature [46–48].

Surface characteristics of materials, such as roughness, hardness, hydrophobicity/hydrophilicity, porosity, can also have a substantial influence for the formation of biofilms of individual strains [48,49]. Pure PLA as a negative control had a relatively smooth surface. Samples with 2, 5 and 10 wt. % PMTABuI showed some surface roughness (Table 2) and surface ionic bonding. The inhibitory effect of the material on the biofilm is then combined. It depends not only on the nature of bacterial adhesion to the material, but especially on the positive charge of nitrogen (N^+) in PMTABuI. It is likely that N^+ binds to the negatively charged bacterial membrane and thereby reduces bacterial viability [21]. The amount of living bacterial cells in biofilms was detected by monitoring their metabolic activities using MTT assay [49,50]. In our study, the PLA+PMTABuI composites effectively decreased viability of all bacteria (Fig. 12b, Table S2, S3). The highest inhibition of metabolic activity was found in the case of PLA+PMTABuI 10 wt.% for *A. baumannii* strain (92 ± 5%). For other bacterial strains, the strong reduction of viability was also detected (*E. coli*88 ± 5% > *S. aureus* 85 ± 4% > MRSA 82 ± 4%).

Developing novel antimicrobial compounds and composite polymers primarily targets strategies for controlling biofilm-associated infections. Attention to bacterial biofilms is also relevant in other fields, such as wastewater treatment and food processing equipment [51,52]. In this study, PLA coatings with PMTABuI demonstrated excellent anti-biofilm activity, making them suitable for the prevention and elimination of bacterial biofilms.

3.2. Stability of films

Finally, the prepared PLA+PMTABuI films were evaluated for their stability in several conditions: in the air, in distilled water, 10 wt. % NaCl solution and in PBS buffer for 72 h. The results were subsequently evaluated using SEM with EDAX mapping focusing on the presence of iodine in individual samples. The results are shown in Fig. S5-S7. As can be seen, the samples are stable in the air, but when using water or other solutions, PMTABuI is washed out from the PLA surface (disappearance of iodine can be seen). Given the intended purpose of this material in medical packaging for hospitals, the stability of the films is satisfactory for single-use. When personnel wear gloves, such packaging is safe to use.

4. Conclusion

PMTABuI particles as antimicrobial surface modifiers were deposited on the surface of PLA films using RESS mode SFT with SC—CO_2 to prepare a material with antimicrobial properties using an environmentally friendly process. Purity of synthesized PMTABuI was confirmed by ^{1}H NMR and GPC methods. The results of TGA and DSC analyses show that PMTABuI does not change depending on the process temperature in SFT process. The presence of PMTABuI in the materials was confirmed by FTIR analysis without the formation of new bonds, indicating physical adsorption onto the PLA surface. SEM and AFM confirmed that supercritical processes change the surface morphology of PLA and that PMTABuI particles are present on the surface. EDX analysis and elemental mapping demonstrated that these particles are composed of PMTABuI, which was confirmed by the presence of iodine. XRD showed that the crystallization of PLA during the SFT process was reduced by the SFT process and PMTABuI coating. This reduction was further confirmed by DSC measurements. Antimicrobial tests demonstrated the inhibitory activity of the material against biofilm formation, with the effectiveness increasing with the amount of PMTABuI. However, it was found that the PMTABuI deposit on the PLA surface, which were prepared by the SFT process, are stable in air but leachable in solutions. The solubility in aqueous solutions is connected with higher hydrophilicity of all PLA+PMTABuI samples. The biggest drawback of this material is the inhomogeneous surface coverage with the antimicrobial component and only physical form of bond on surface, and thus the slightly variable properties of the materials. Therefore, further research will be focused on optimizing and homogenizing this process. In this study, there is an obvious limitation to the applicability of the material. Better applicability would be achieved by chemically attaching PMTABuI to the PLA surface, which would be more efficient in terms of utilization. However, this approach would require the use of additional chemicals in the SFT process, which may be less associated with “green chemistry” and would require a more complex manufacturing process. The aim of this article was to present a simple procedure for the preparation of an antimicrobial material. The advantage of the material prepared in this way is its

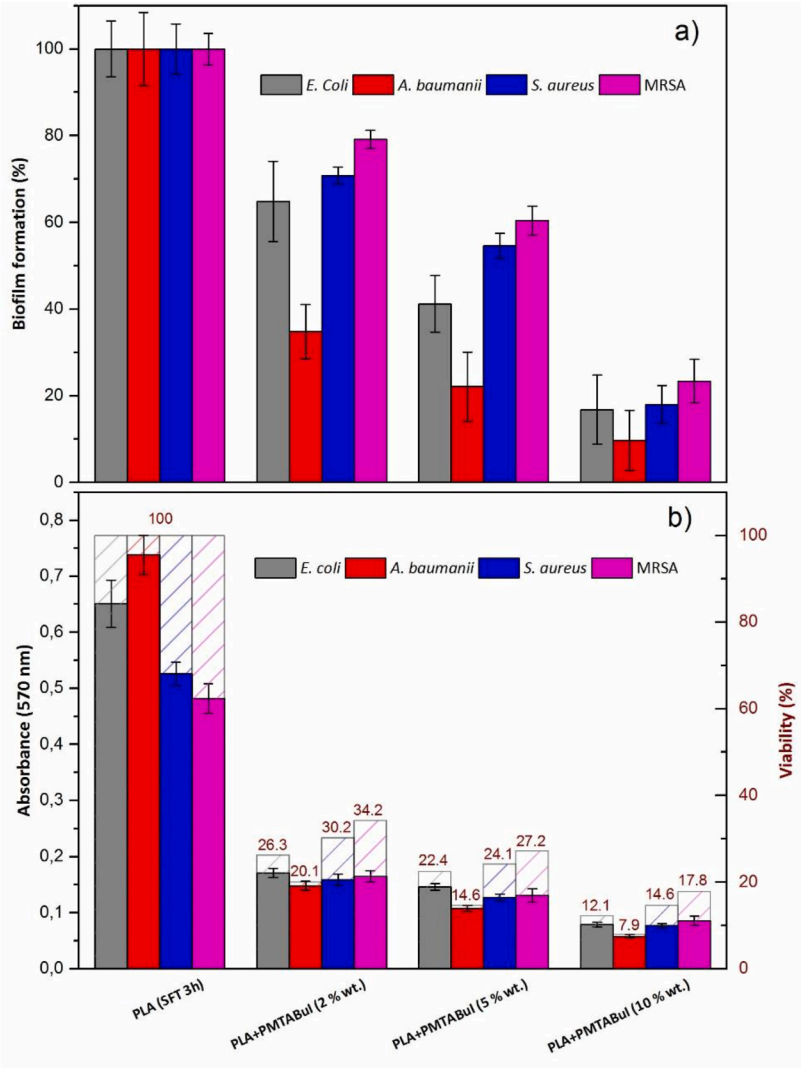

Fig. 12. a) Inhibitory effect of PLA+PMTABuI coatings (2, 5, 10 wt. %) on biofilm formation, PLA (SFT 3 h) – PLA mat cured with SC—CO_2 for 3 h, b) The effect of PLA+PMTABuI coatings(2, 5, 10 wt. %) on bacterial biofilm viability (black – measured absorbance of viable cells, dark red and cross hatched – evaluated viability of cells).

easier recyclability due to the subsequent easy separation of PMTABuI and PLA for further processing.

The semi-crystalline antimicrobial materials prepared in this work, intentionally derived from amorphous PLA, was intentionally designed for use in hospital packaging. The transformation from the amorphous state to the semi-crystalline form during impregnation with antimicrobial PMTABuI by SFT underlines its suitability for more rigid packaging requirements. The antimicrobial properties of this material can significantly contribute to prolonging the sterilization efficiency of devices placed in these containers. Variations in the amount of PMTABuI and optimization of the SFT process can lead to a material with a more amorphous form that could be equally suitable for use in hospital packaging. This flexibility allows the material properties to be tailored to specific packaging needs, whether the rigidity of semi-crystalline PLA or the flexibility and optical clarity of amorphous PLA are required. Thus, by adjusting these parameters, the material can be tailored to enhance its performance.

Funding

This study was supported by project No CZ.02.01.01/00/22_008/0004631. "Materials and technologies for sustainable development" within the Jan Amos Komensky Operational Program financed by the European Union and from the state budget of the Czech Republic, and the financial support of the European Union under the REFRESH – Research Excellence For REgion Sustainability and High-tech Industries project number CZ.10.03.01/00/22_003/0000048 via the Operational Programme Just Transition. This study was also supported in „Advanced Materials for Energy and Environmental Technologies"project, reg. nr. CZ.02.01.01/00/23_021/0008592 within the Programme Johannes Amos Comenius. " . This work is also part of the project PID2022–136516OB-I00 founded by MCIN/AEI/10.13039/501,100,011,033/FEDER, UE.

CRediT authorship contribution statement

Jakub Zágora: Writing – original draft, Investigation, Formal analysis, Data curation, Methodology, Visualization, Writing – review & editing. **Zuzana Rybková:** Writing – original draft, Methodology, Investigation, Data curation, Formal analysis. **Kateřina Škrlová:** Validation, Supervision, Visualization, Writing – original draft. **Kateřina Malachová:** Writing – original draft, Methodology, Visualization. **Alexandra Muñoz-Bonilla:** Validation, Investigation, Formal analysis. **Marta Fernández-Garcia:** Writing – original draft, Supervision,

Methodology, Conceptualization, Formal analysis. **Daniela Plachá:** Conceptualization, Funding acquisition, Methodology, Supervision, Validation, Writing – original draft, Writing – review & editing.

Declaration of competing interest

The authors declare that they have no known competing financial interests or personal relationships that could have appeared to influence the work reported in this paper.

Acknowledgement

The authors would like to thank P. Peikertová for the FTIR measurements, R. Gábor and M. Heliová for the SEM AFM measurements, and M. Hundáková for the XRD measurements.

Supplementary materials

Supplementary material associated with this article can be found, in the online version, at doi:10.1016/j.rineng.2026.110648.

Data availability

Data will be made available on request.

References

[1] Y. Fu, E.G. Dudley, Antimicrobial-coated films as food packaging: a review, Compr. Rev. Food Sci. Food Saf. 20 (2021) 3404–3437, https://doi.org/10.1111/1541-4337.12769.
[2] A. Tiwari, Handbook of Antimicrobial Coatings, Elsevier, 2018, https://doi.org/10.1016/C2016-0-01441-9.
[3] A. Shahid, B. Aslam, S. Muzammil, N. Aslam, M. Shahid, A. Almatroudi, et al., The prospects of antimicrobial coated medical implants, J. Appl. Biomater. Funct. Mater. 19 (2021), https://doi.org/10.1177/22808000211040304.
[4] H.J. Busscher, H.C. Van Der Mei, G. Subbiahdoss, P.C. Jutte, J.J.A.M. Van Den Dungen, S.A.J. Zaat, et al., Biomaterial-associated infection: locating the finish line in the race for the surface, Sci. Transl. Med. 4 (2012), https://doi.org/10.1126/scitranslmed.3004528.
[5] D. Campoccia, L. Montanaro, C.R. Arciola, A review of the biomaterials technologies for infection-resistant surfaces, Biomaterials 34 (2013) 8533–8554, https://doi.org/10.1016/j.biomaterials.2013.07.089.
[6] Y. Xue, H. Xiao, Y. Zhang, Antimicrobial polymeric materials with quaternary ammonium and phosphonium salts, Int. J. Mol. Sci. 16 (2015) 3626–3655, https://doi.org/10.3390/ijms16023626.
[7] A. Chiloeches, J. Zágora, D. Plachá, M.D.T. Torres, C. de la Fuente-Nunez, F. López-Fabal, et al., Synergistic combination of antimicrobial peptides and cationic polyitaconates in multifunctional PLA fibers, ACS. Appl. Bio Mater. 6 (2023) 4805–4813, https://doi.org/10.1021/acsabm.3c00576.
[8] A. Chiloeches, C. Echeverría, R. Cuervo-Rodríguez, D. Plachà, F. López-Fabal, M. Fernández-García, et al., Adhesive antibacterial coatings based on copolymers bearing thiazolium cationic groups and catechol moieties as robust anchors, Prog. Org. Coat. 136 (2019) 105272, https://doi.org/10.1016/j.porgcoat.2019.105272.
[9] I. Zizovic, Supercritical fluid applications in the design of novel antimicrobial materials, Molecules 25 (2020) 2491, https://doi.org/10.3390/molecules25112491.
[10] Q. Su, Y. Xue, C. Wang, Q. Zhou, Y. Zhao, J. Su, et al., Strategies and applications of antibacterial surface-modified biomaterials, Bioact. Mater. 53 (2025) 114–140, https://doi.org/10.1016/j.bioactmat.2025.07.009.
[11] D.J. da Silva, G.S. Ferreira, A. Duran, F.L.A. Fonseca, R.F. Bueno, D.S. Rosa, Super effective antimicrobial silver-sputtered coatings on poly(lactic acid) against bacteria and omicron SARS-CoV-2, Mater. Today Chem. 30 (2023) 101481, https://doi.org/10.1016/j.mtchem.2023.101481.
[12] A. Nirmala, S. Pottath, A.V. Prasannakumari, V.R. Gnanaraj, J. Jacob, B.S. D. Kumar, et al., Oxide anchored multi-charged metal complexes with binary nanoparticles for stable and efficient anti-bacterial coatings on cotton fabrics, Mater. Adv. 4 (2023) 6213–6222, https://doi.org/10.1039/d3ma00605k.
[13] A.Z. Chen, Z. Zhao, S.B. Wang, Y. Li, C. Zhao, Y.G Liu, A continuous RESS process to prepare PLA-PEG-PLA microparticles, J. Supercrit. Fluids. 59 (2011) 92–97, https://doi.org/10.1016/j.supflu.2011.08.012.
[14] M.A.E. Sayed, N.T. Elazab, M. Gassoumi, M.A.M. Ibrahim, Nanocrystalline silver coatings on steel by electrodeposition from non-polluting aqueous baths and its antibacterial activity, J. Taiwan. Inst. Chem. Eng. 132 (2022) 104212, https://doi.org/10.1016/j.jtice.2022.104212.
[15] A.H.M. Abd El-Gawad, A.A.I. Khalil, A.S Gadallah, Influence of preparation conditions on the properties of silver doped copper-zinc sulfide thin films prepared via sol-gel spin coating technique, Optik 223 (2020) 165561, https://doi.org/10.1016/j.ijleo.2020.165561.
[16] Y. Wang, S. Shang, L.K. Chiu, S. Jiang, Mimicking Saharan silver ant's hair: a bionic solar heat shielding architextile with hexagonal ZnO microrods coating, Mater. Lett. 261 (2020) 127013, https://doi.org/10.1016/j.matlet.2019.127013.
[17] C. Muñoz-Nuñez, V. Hevilla, E. Blázquez-Blázquez, J. Zagora, D. Placha, A. Muñoz-Bonilla, et al., Functionalization of chitosan films using essential oils by supercritical CO2 impregnation method for various applications, Carbohydr. Polym. Technol. Appl. 8 (2024) 100559, https://doi.org/10.1016/j.carpta.2024.100559.
[18] A.R.C. Duarte, M.S. Costa, A.L. Simplício, M.M. Cardoso, C.M.M. Duarte, Preparation of controlled release microspheres using supercritical fluid technology for delivery of anti-inflammatory drugs, Int. J. Pharm. 308 (2006) 168–174, https://doi.org/10.1016/j.ijpharm.2005.11.012.
[19] D. Plachá, P. Stuchlík, O. Dutko, T. Sosna, M. Mikeska, Supercritical fluid extraction as a method for preparation of submicron particles of cimetidine and hydrochlorothiazide, Adv. Sci. Lett. 22 (2016) 670–674, https://doi.org/10.1166/asl.2016.6988.
[20] K. Škrlová, Z. Rybková, T. Stachurová, J. Zagora, K. Malachová, D. Měřinská, et al., Long-term antimicrobial effect of polylactide-based composites suitable for biomedical use, Polym. Test. 116 (2022), https://doi.org/10.1016/j.polymertesting.2022.107760.
[21] R. Tejero, D. López, F. López-Fabal, J.L. Gómez-Garcés, M. Fernández-García, Antimicrobial polymethacrylates based on quaternized 1,3-thiazole and 1,2,3-triazole side-chain groups, Polym. Chem. 6 (2015) 3449–3459, https://doi.org/10.1039/c5py00288e.
[22] R. Tejero, D. López, M. Fernández-García, Influence of spacer group on the structure and thermal properties of copolymers based on acrylonitrile and methacrylic 1,3-thiazole and 1,2,3-triazole derivatives, Eur. Polym. J. 71 (2015) 401–411, https://doi.org/10.1016/j.eurpolymj.2015.08.014.
[23] D. Plachá, A. Muñoz-Bonilla, K. Škrlová, C. Echeverria, A. Chiloeches, M. Petr, et al., Antibacterial character of cationic polymers attached to carbon-based nanomaterials, Nanomaterials 10 (2020) 1–14, https://doi.org/10.3390/nano10061218.
[24] S. Pérez-Davila, L. González-Rodríguez, R. Lama, M. López-Álvarez, A.L. Oliveira, J. Serra, et al., 3D-Printed PLA medical devices: physicochemical changes and biological response after sterilisation treatments, Polymers 14 (2022) 1–20, https://doi.org/10.3390/polym14194117.
[25] V. DeStefano, S. Khan, A. Tabada, Applications of PLA in modern medicine, Eng. Regen. 1 (2020) 76–87, https://doi.org/10.1016/j.engreg.2020.08.002.
[26] D. Srikanth, S.V. Joshi, M. Ghouse Shaik, G. Pawar, S. Bujji, V. Kanchupalli, et al., A comprehensive review on potential therapeutic inhibitors of nosocomial Acinetobacter baumannii superbugs, Bioorg. Chem. 124 (2022) 105849, https://doi.org/10.1016/j.bioorg.2022.105849.
[27] X. Wu, H. Wang, J. Xiong, G.X. Yang, J.F. Hu, Q. Zhu, et al., Staphylococcus aureus biofilm: formulation, regulatory, and emerging natural products-derived therapeutics, Biofilm 7 (2024) 100175, https://doi.org/10.1016/j.bioflm.2023.100175.
[28] C. Rossi, C. Chaves-López, A. Serio, E. Goffredo, B.C. Goga, A. Paparella, Influence of incubation conditions on biofilm formation by pseudomonas fluorescens isolated from dairy products and dairy manufacturing plants, Ital. J. Food Saf. 5 (2016), https://doi.org/10.4081/ijfs.2016.5793.
[29] R. Kamimura, H. Kanematsu, A. Ogawa, T. Kogo, H. Miura, R. Kawai, et al., Quantitative analyses of biofilm by using crystal violet staining and optical reflection, Materials 15 (2022), https://doi.org/10.3390/ma15196727.
[30] T. Stachurová, Z. Rybková, K. Škrlová, K. Malachová, M. Havlíček, D. Plachá, Biocompatibility and biocidal effects of modified polylactide composites, Front. Microbiol. 13 (2022) 1–15, https://doi.org/10.3389/fmicb.2022.1031783.
[31] T. Mosmann, Rapid colorimetric assay for cellular growth and survival: application to proliferation and cytotoxicity assays, J. Immunol. Methods 65 (1983) 55–63, https://doi.org/10.1016/0022-1759(83)90303-4.
[32] K. Škrlová, K. Malachová, A. Muñoz-Bonilla, D. Měřinská, Z. Rybková, M. Fernández-García, et al., Biocompatible polymer materials with antimicrobial properties for preparation of stents, Nanomaterials 9 (2019), https://doi.org/10.3390/nano9111548.
[33] A. Muñoz-Bonilla, J. Zagora, D. Plachá, C. Echeverría, A. Chiloeches, M. Fernández-García, Chemical hydrogels bearing thiazolium groups with a broad spectrum of antimicrobial behavior, Polymers 12 (2020) 1–11, https://doi.org/10.3390/polym12122853.
[34] M. Mu, S. Liu, W. DeFlorio, L. Hao, X. Wang, K.S. Salazar, et al., Influence of surface roughness, nanostructure, and wetting on bacterial adhesion, Langmuir 39 (2023) 5426–5439, https://doi.org/10.1021/acs.langmuir.3c00091.
[35] K. Yang, J. Shi, L. Wang, Y. Chen, C. Liang, L. Yang, et al., Bacterial anti-adhesion surface design: surface patterning, roughness and wettability: a review, J. Mater. Sci. Technol. 99 (2022) 82–100, https://doi.org/10.1016/j.jmst.2021.05.028.
[36] A. Muñoz-bonilla, L. Daniel, M. Fern, Providing antibacterial activity to poly (2-hydroxy ethyl methacrylate) by copolymerization with a methacrylic thiazolium derivative, 2018, https://doi.org/10.3390/ijms19124120.
[37] J.D. Badia, L. Santonja-Blasco, A. Martínez-Felipe, A. Ribes-Greus, Hygrothermal ageing of reprocessed polylactide, Polym. Degrad. Stab. 97 (2012) 1881–1890, https://doi.org/10.1016/j.polymdegradstab.2012.06.001.
[38] P. Shree, C.K. Singh, K.K. Sodhi, J.N. Surya, D.K. Singh, Biofilms: understanding the structure and contribution towards bacterial resistance in antibiotics, Med. Microecol. 16 (2023) 100084, https://doi.org/10.1016/j.medmic.2023.100084.
[39] R. Gattu, S.S. Ramesh, S. Ramesh, Role of small molecules and nanoparticles in effective inhibition of microbial biofilms: a ray of hope in combating microbial resistance, Microb. Pathog. 188 (2024) 106543, https://doi.org/10.1016/j.micpath.2024.106543.

[40] V.C. Kalia, S.K.S. Patel, J.K. Lee, Bacterial biofilm inhibitors: an overview, Ecotoxicol. Environ. Saf. 264 (2023) 115389, https://doi.org/10.1016/j.ecoenv.2023.115389.
[41] C. Wilson, R. Lukowicz, S. Merchant, H. Valquier-Flynn, J. Caballero, J. Sandoval, et al., Quantitative and qualitative assessment methods for biofilm growth: a mini-review, Res. Rev. J. Eng. Technol. 6 (2017).
[42] H.J. Mea, P.V.C. Yong, E.H. Wong, An overview of Acinetobacter baumannii pathogenesis: motility, adherence and biofilm formation, Microbiol. Res. 247 (2021) 126722, https://doi.org/10.1016/j.micres.2021.126722.
[43] K. Upmanyu, Q.M.R. Haq, R. Singh, Factors mediating Acinetobacter baumannii biofilm formation: opportunities for developing therapeutics, Curr. Res. Microb. Sci. 3 (2022) 100131, https://doi.org/10.1016/j.crmicr.2022.100131.
[44] R. Ruhal, R. Kataria, Biofilm patterns in gram-positive and gram-negative bacteria, Microbiol. Res. 251 (2021) 126829, https://doi.org/10.1016/j.micres.2021.126829.
[45] G.J. Jeong, F. Khan, N. Tabassum, K.J. Cho, Y.M. Kim, Controlling biofilm and virulence properties of gram-positive bacteria by targeting wall teichoic acid and lipoteichoic acid, Int. J. Antimicrob. Agents 62 (2023) 106941, https://doi.org/10.1016/j.ijantimicag.2023.106941.
[46] J. Yang, F. Jia, Y. Qiao, Z. Hai, X. Zhou, Correlation between bacterial extracellular vesicles and antibiotics: a potentially antibacterial strategy, Microb. Pathog. 181 (2023) 106167, https://doi.org/10.1016/j.micpath.2023.106167.
[47] G.J. Jeong, F. Khan, N. Tabassum, K.J. Cho, Y.M. Kim, Bacterial extracellular vesicles: modulation of biofilm and virulence properties, Acta Biomater. 178 (2024) 13–23, https://doi.org/10.1016/j.actbio.2024.02.029.
[48] X. Nie, Q. Li, X. Chen, S. Onyango, J. Xie, S. Nie, Bacterial extracellular vesicles: vital contributors to physiology from bacteria to host, Microbiol. Res. 284 (2024) 127733, https://doi.org/10.1016/j.micres.2024.127733.
[49] J. Qi, M. Gong, R. Zhang, Y. Song, Q. Liu, H. Zhou, et al., Evaluation of the antibacterial effect of tea tree oil on Enterococcus faecalis and biofilm in vitro, J. Ethnopharmacol. 281 (2021) 114566, https://doi.org/10.1016/j.jep.2021.114566.
[50] C. Wang, P.W. Wei, C.R. Song, X. Wang, G.F. Zhu, Y.X. Yang, et al., Evaluation of the antimicrobial function of Ginkgo biloba exocarp extract against clinical bacteria and its effect on Staphylococcus haemolyticus by disrupting biofilms, J. Ethnopharmacol. 298 (2022) 115602, https://doi.org/10.1016/j.jep.2022.115602.
[51] Y. Bi, G. Xia, C. Shi, J. Wan, L. Liu, Y. Chen, et al., Therapeutic strategies against bacterial biofilms, Fundam. Res. 1 (2021) 193–212, https://doi.org/10.1016/j.fmre.2021.02.003.
[52] Y.J. Park, C.E. Kang, J.H. Kim, D. Shin, D.H. Lee, N.K. Lee, et al., Antibacterial mechanism of mixed natural preservatives (ε-poly-lysine, cinnamon extract, and chestnut inner shell extract) against Listeria monocytogenes, LWT 177 (2023) 114572, https://doi.org/10.1016/j.lwt.2023.114572.